Available online at www.sciencedirect.com
ScienceDirect
Journal of Catalysis 251 (2007) 113–122
JOURNAL OF CATALYSIS
www.elsevier.com/locate/jcat

Lanthanum oxides for the selective synthesis of phytosterol esters: Correlation between catalytic and acid–base properties

S. Valange [a,*], A. Beauchaud [a], J. Barrault [a], Z. Gabelica [b], M. Daturi [c], F. Can [c]

[a] *LACCO, UMR CNRS 6503, ESIP, 40 Av. Recteur Pineau, F-86022 Poitiers Cedex, France*
[b] *Université de Haute-Alsace, ENSCMu, GSEC, 3 rue A. Werner, F-68093 Mulhouse Cedex, France*
[c] *LCS, UMR CNRS 6506, ENSICAEN, 6 boulevard Maréchal Juin, F-14050 Caen Cedex, France*

Received 20 April 2007; revised 5 July 2007; accepted 7 July 2007

Available online 20 August 2007

Abstract

The selective synthesis of phytosterol esters from natural sterols and methyl esters was investigated on new grounds by a chemical process using basic solids that are reusable, active, and more selective than the currently used homogeneous catalysts (e.g., alkali hydroxides, carbonates). Various lanthanum oxides with different synthesis procedures and varying specific surface areas were tested. The catalytic performance of the new solids and, more specifically, the ability of La_2O_3 oxides in increasing phytosterol ester selectivity, was correlated with their acido-basic properties, which were fully characterized by infrared spectroscopy. All La_2O_3 oxides involved surface carbonate species with different structural states and strengths, as revealed by propyne adsorption. The selectivity to phytosterol ester varied from 90 to 96%, confirming that the side reaction of dehydration of β-sitosterol was strongly inhibited. The phytosterol ester yield could reach 89% and was related to the basic strength of the carbonate species. The lower the carbonate basicity, the higher the phytosterol ester yield. Moreover, IR spectra of catalysts diluted in KBr powder showed that the higher the intensity of unidentate carbonate bands, the higher the yield. It was concluded that the synthesis of phytosterol esters from fatty methyl esters and sitosterols in the presence of La_2O_3 catalysts requires ionic carbonate species of medium basic strength.

Keywords: Selective synthesis of phytosterol esters; Lanthanum oxides; Lanthanum oxycarbonates; Basicity; Propyne adsorption; Infrared spectroscopy

1. Introduction

Basic solid materials are of great importance in heterogeneous catalysis if the nature, quantity, distribution, and strength of the basic sites can be monitored so as to yield active centers well adapted to a particular catalytic reaction. The characterization of these sites requires specific techniques, such as IR spectroscopy of adsorbed probe molecules, as well as gravimetric and calorimetric adsorption of CO_2.

In numerous chemical reactions starting from alcohols, esters, or acids, strong mineral or organic bases (e.g., KOH, NaOEt) are currently used [1–4], but the corrosive character of homogeneous catalysts and the difficulty in separating them from the reaction medium make them less well suited for environmentally friendly catalytic processes. Moreover, such strong bases also can favor the formation of byproducts as a consequence of dehydration, polymerization, oxidation, and other side reactions, resulting in decreased selectivity toward the desired compounds. As an example, transesterification reactions using solid base catalysts provide an attractive alternative by avoiding these drawbacks, because they are easily recovered (through simple filtration) and recycled.

Phytosterol esters are useful in food applications [5] and in other areas, such as cosmetics [6]. Pouilloux et al. [7] have previously shown that basic solids, such as magnesium or zinc oxides, can be advantageously used in the transesterification of sitosterols with fatty methyl esters in the absence of any solvent. A phytosterol ester yield >75% was obtained, despite the fact that acid sites, also present on MgO in high amounts along with the strong basic sites, favor the formation of stigmastadienes through a dehydration side reaction.

* Corresponding author. Fax: +33 5 49 45 33 49.
E-mail address: sabine.valange@univ-poitiers.fr (S. Valange).

0021-9517/$ – see front matter
doi:10.1016/j.jcat.2007.07.004

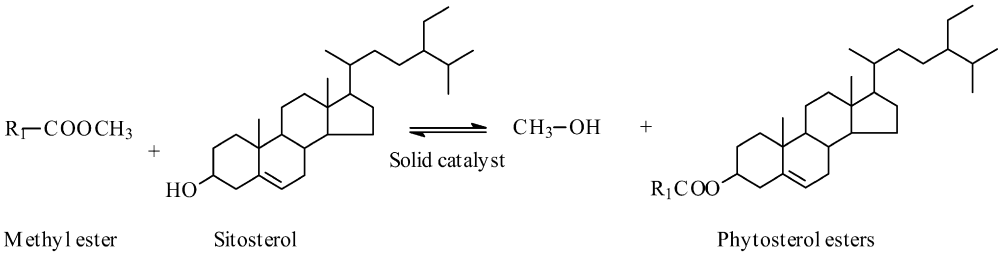

Fig. 1. Reaction scheme for phytosterol esters selective synthesis.

The aim of this work was to study the synthesis of phytosterol esters through the transesterification of β-sitosterol with methyl dodecanoate (Fig. 1) in the presence of less conventional basic solid catalysts, such as lanthanum oxides prepared using different synthetic routes and involving variable specific surface areas. Lanthanum oxide has found numerous applications in environmental chemistry and exhibits interesting versatility in catalytic reactions. As a recent example, lanthanum oxide was used to catalyze the reduction of NO by methane in the presence of oxygen [8,9]. Most of the studies dealing with catalysis over rare earth oxides have found that the basic character of such materials was an important factor in determining the reaction mechanism. The fact that the basic character of lanthanum oxide depends markedly on its structural or textural properties, which are in turn sensitive to its synthesis and pretreatment conditions, have justified numerous studies devoted exclusively to less conventional preparation routes that eventually yield rare earth oxide materials with specific properties. For instance, Lacombe et al. [10] derived a relationship between the morphology and catalytic performance of La_2O_3 for the methane oxidative coupling reaction. The basic character of La oxides is much better demonstrated by the calorimetric adsorption of CO_2 reported by Auroux and Gervasini [11] or Veldurthy et al. [12]. The catalytic properties for well-established base-catalyzed reactions, such as Michael [13] and transesterification [14] reactions, are also known. Lanthanum oxide is well known to be very sensitive to water and to atmospheric CO_2, leading to its bulk hydroxylation and/or the formation of various superficial carbonate species [15]. As shown by Klingenberg et al. [16], the surface chemistry of commercial lanthanum carbonate and oxide powders was shown to be greatly influenced by the pretreatment conditions (e.g., calcination, exposure to water) that define the final surface state of the materials. Turcotte et al. [17] have shown that IR spectroscopy can discriminate between three different polymeric forms of $La_2O_2CO_3$, thereby suggesting that IR is the most efficient technique for characterizing the structure of carbonate-like species.

The main purpose of the present study was to evaluate the ability of La_2O_3 oxides prepared using the so-called "self-combustion" method to increase the catalytic performance (activity and selectivity) for the synthesis of phytosterol esters in comparison with more conventional basic solids currently used and, in a further step, to identify the active species and their basic strength. La_2O_3 acid–base properties were studied by IR spectroscopy by using pyridine (surface acidity) and propyne (surface basicity) as probe molecules.

Table 1
Specific surface area of lanthanum oxides and their initial rate during the synthesis of phytosterol esters from methyl dodecanoate and β-sitosterol

Catalyst [a]	S_{BET} ($m^2\,g^{-1}$)	Activity[b] ($mmol\,h^{-1}\,g^{-1}$)
Sample 1	68	39
Sample 2	1	32
Sample 3	3	50
Sample 4	40	55

[a] Samples 1 to 3 were supplied by Rhodia and sample 4 was prepared by the self combustion method.
[b] Temperature 513 K, reaction time 7 h, $D_{N_2} = 15\ mL\,min^{-1}$, ester/sterol molar ratio = 1, catalyst = 2.2 wt%.

2. Experimental

2.1. Catalyst preparation

Lanthanum oxide (herewith referred as sample 4) was prepared by the self-combustion method [18]. Glycine (H_2NCH_2–CO_2H) was used as the ignition promoter and was added to an aqueous solution of lanthanum nitrate (NO_3^-/NH_2 molar ratio = 1). The resulting solution was slowly evaporated until a vitreous gel was obtained. The latter was heated up to 523 K, the temperature at which the ignition reaction occurs. This rapid exothermic reaction resulted in formation of a white powdery solid. Three other commercial lanthanum oxides supplied by Rhodia (samples 1, 2, and 3) exhibiting different specific surface areas (Table 1) were used for comparison.

2.2. Characterization

La_2O_3 samples were characterized by powder X-ray diffraction using a Bruker D5005 diffractometer with monochromatized Cu$K\alpha$ radiation ($\lambda = 1.5418$ Å) at 40 kV and 30 mA. The diffraction patterns were recorded in the 2θ value range of 10–90° at a rate of $0.04°\,s^{-1}$ and a step size of 2 s. The BET surface areas were determined by adsorption–desorption of nitrogen on a Micromeritics Flowsorb II 2300 apparatus at 77 K. Before each experiment, the samples were degassed under He at 623 K for 30 min before adsorption of nitrogen using 30% N_2/Ar as the adsorbate.

2.3. IR spectroscopy

IR spectra were recorded on a Nicolet Nexus spectrometer with a spectral resolution of 4 cm^{-1}. Samples were pressed as

self-supported wafers. Discs of 10 mg cm^{-2} were prepared and treated directly in the cell. The samples were first evacuated up to 623 K (10.8 K min^{-1}) then treated under 100 Torr of oxygen for 30 min before being evacuated for another 30 min at 623 K and then up to 873 K (8.3 K min^{-1}). At the latter temperature, the samples were further treated under 100 Torr of oxygen for 1 h, then evacuated for 30 min. Probe molecules (pyridine and propyne) were introduced on the activated samples at room temperature. To analyze the structure of lanthanum oxycarbonates, spectra were recorded on wafers containing sample powder diluted in KBr.

2.4. Catalytic tests

The transesterification of β-sitosterol with methyl dodecanoate was carried out at atmospheric pressure under a nitrogen flow in a Pyrex reactor equipped with a mechanical stirrer. First, 7.7×10^{-3} mol of sterol (3.2 g) and 7.7×10^{-3} mol of methyl dodecanoate (1.64 g) were heated to 513 K, then 125 mg of catalyst (2.2 wt%) were added to the mixture (starting time of the reaction). The analysis of the reaction products was performed on a gas chromatograph equipped with a flame ionization detector and an on-column injector with flowing N_2 as carrier gas. The percentage of each compound was determined using hexadecane as an internal standard. The conversions of methyl dodecanoate and β-sitosterol were followed as functions of the time on stream of the microsamples withdrawn periodically and evaluated with respect to the initial and final contents of fatty methyl ester and free sterol in the solution.

3. Results and discussion

3.1. Catalyst characterization

The XRD pattern obtained for lanthanum oxide as prepared by the self-combustion method (sample 4) showed only the diffraction lines expected for La_2O_3, which are broadened due to the very small particle size. No other diffraction lines due to possible residual La nitrate were visible, confirming that the autoignition temperature of the homogeneous intermediate material (which combusts to generate the final powder) was fully achieved. It has been reported [18] that the self-combustion temperature of an intermediate product formed from lanthanum nitrate hydrate is about 473 K, which can be easily achieved on a heating plate. This was also confirmed by achieving the self-combustion reaction using a thermoanalytical instrument (TG-DTA trace not shown).

A closer look at the diffraction pattern, along with thermal analysis and preliminary IR characterization data, indicated the presence of residual carbonate species inside this product. In fact, surface carbonate species were detected in both sample 4 and in the samples supplied by Rhodia (samples 1–3). It is well known that rare earth oxides, particularly La_2O_3, undergo rapid (partial) carbonation through reacting with atmospheric carbon dioxide. This effect can be even more pronounced when La_2O_3 is synthesized by autoignition, because combustion of the amino acid generates CO_2 in situ.

The specific surface area of the various lanthanum oxides is given in Table 1. The surface area of sample 4 was relatively high (40 $m^2\,g^{-1}$), in line with the synthesis procedure yielding a fine metal oxide powder with high specific surface area, due to short reaction time and low synthesis temperature. Two of the other three commercial La_2O_3 oxides exhibited very low surface areas, whereas sample 1 had the highest surface value reported for that compound (68 $m^2\,g^{-1}$). To prepare a high-surface area La_2O_3 via the autoignition process, we selected two lanthanum precursor salts (acetate and sulphate); we also studied other combustible/soluble metal salt ratios using La nitrate. The best product was generally obtained when the glycine-to-anion molar ratio was adjusted to produce the largest bulk volume of powder. However, whatever the experimental conditions, we could never prepare lanthanum oxide with surface area >40 $m^2\,g^{-1}$. In this study, the favorable conditions for generating La_2O_3 are typically a glycine-to-anion ratio of 1 with lanthanum nitrate hydrate as a precursor salt.

3.2. IR characterization of La_2O_3 samples

The effect of activation on IR spectra of various lanthanum oxides catalysts is reported on Fig. 2. Before activation, the IR spectrum of samples 1–3 in the ν(OH) range displayed two bands at 3595 and 3452 cm^{-1} (Fig. 2A). According to Mekhemer [19] and Laachir et al. [20], the band at 3595 cm^{-1} is due to tridentate OH groups linked to La^{3+} cations. The band at 3452 cm^{-1} is assigned to the ν(OH) vibration mode of adsorbed water. The corresponding δ(OH) bending mode is observed at 1630 cm^{-1} [21,22]. For sample 4, a broad massif assigned to hydrogen-bonded water was observed over the range of the OH group stretching modes.

In all spectra, at lower wavenumbers, strong bands were present in the ν(OCO) vibration range (1200–1650 cm^{-1}). In agreement with previous studies [23], these bands are assigned to carbonate species. However, because of excessively high intensity (leading to saturation of the detector), these bands could not be analyzed in detail. Fig. 2B shows the IR spectra of lanthanum oxide samples activated at 873 K under oxygen. In this case, activation resulted in the total removal of adsorbed water but did not lead to complete elimination of carbonate groups, as was reported previously [24]. The removal of part of carbonate species allowed us to conclude that the CO_3^{2-} groups in the various samples had different structures, as demonstrated by the different IR bands shown in Fig. 2B. It is known that lanthanum cations easily form carbonate-like species such as $La(OH)(CO_3)$ [25]. Thermal treatments lead to a partial transformation of these species to oxy-carbonate ($La_2O_2CO_3$) and finally to La_2O_3. These decompositions require temperatures of 773–973 K to generate $La_2O_2CO_3$ and 1073 K or above to form the oxide [16]. An important result is that this final step is reversible in CO_2-containing atmospheres [17].

In a previous work, Turcotte et al. [17] found three different polymeric forms of $La_2O_2CO_3$, distinguished by their IR spectra: tetragonal type I, monoclinic type Ia, and hexagonal type II phases. The corresponding IR spectra in the ν(OCO) vibration range often display a complex band structure due to the

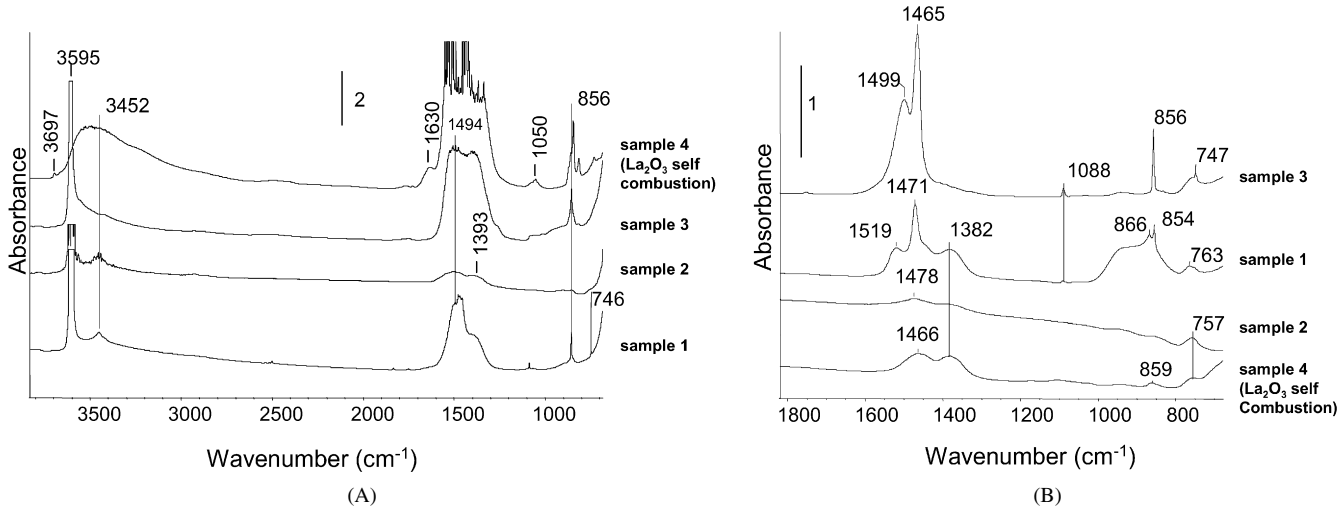

Fig. 2. Effect of activation temperature on IR spectra of samples 1 to 4: (A) samples before activation; (B) samples after activation at 873 K under oxygen.

presence of the different polymeric forms currently present on the La_2O_3 surface, which is also expected in our case. A "free" carbonate, corresponding to a symmetric structure, is characterized by a doubly degenerated asymmetric stretching band at ~1415–1450 cm^{-1}. It has been considered that the $\Delta\nu_3$ splitting of this degenerated ν_3 vibration should selectively characterize each species structure [26]. According to the literature [17,27], the splitting of the ν_3 mode is far more pronounced for the carbonate structures I and Ia with respect to that commonly observed for mineral carbonates (type II). In our case, after the thermal treatment at 873 K under O_2, only the most stable carbonate species were present on the surface of lanthanum oxides. The sharp bands at 1471 and 1465 cm^{-1} observed on spectra of samples 1 and 3 characterize these carbonates, and the narrow $\Delta\nu_3$ interval between these frequencies suggest that we indeed are dealing with mineral (hexagonal) type II $La_2O_2CO_3$ species. Sample 2 showed a similar band at 1478 cm^{-1}, substantially weaker than for the other two compounds, revealing the presence of traces of carbonates of the same species. Polydentate carbonates were also observed, especially on sample 1 (bands at 1519 and 1382 cm^{-1}). Interestingly, sample 4 showed only bands assigned to polydentate carbonates at 1466 and 1382 cm^{-1}. The corresponding ν_1 and $\pi(CO_3)$ modes for all the carbonates were observed at 1080 cm^{-1} (more intense on sample 4) and around 850 cm^{-1} (all samples), respectively. In addition, sample 1 revealed combination bands of La–O fundamental vibrational modes at around 940–920 cm^{-1}. This broad band was far more pronounced on this catalyst due to its relatively high specific surface area.

This preliminary IR characterization of the various lanthanum oxycarbonate solids indicates the presence of very different surface and structural states, auguring different catalytic behaviors. Varying the specific surface area even within the same synthesis procedure also strongly modified the chemical and superficial states of the materials. Finally, this preliminary screening did not allow us to detect the other, more labile carbonate species that had disappeared at the activation temperatures and that could potentially play a major role as active (basic) species during the catalysis done at lower temperatures. Thus, additional investigations were necessary, as reported below.

3.3. Selective synthesis of phytosterol esters

3.3.1. Influence of specific surface area on catalytic activity and IR characterization of KBr-diluted samples

The initial rates of methyl dodecanoate transesterification with β-sitosterol in the presence of the various La_2O_3 samples are presented in Table 1. Surprisingly, no direct correlation could be found between the surface area (S_{BET}) of the samples and the catalytic activity extrapolated at zero conversion. Comparison of samples 1 and 2, which have very different surface areas (S_{BET} of 68 and 1 $m^2\,g^{-1}$, respectively), indicates a negligible effect of S_{BET} on the catalytic performance, with similar initial reaction rates. These unexpected results suggest that the main parameter affecting the activities can be related to the acid–base properties of the samples and, more specifically, to the nature of the active basic sites of the various lanthanum oxides, which is different, as confirmed by the preliminary IR characterization.

We achieved a more in-depth investigation of the basic properties of the different samples by diluting the powders into KBr pellets (1 wt%). Besides preventing the detector saturation, this technique proved more efficient for analyzing all carbonate species originally present on the surface before evacuation. Indeed, a severe thermal treatment (873 K under O_2) would inevitably result in the removal of the less stable carbonate species (often the most reactive), thereby preventing identification of their structure (symmetry), a parameter that dramatically influences reactivity. The KBr dilution method should accurately identify the most active species under (spectral) conditions similar to those encountered during catalytic tests (513 K).

Spectra in the 1700–1200 cm^{-1} range of the four samples diluted in KBr, presented in Fig. 3, confirm that these catalysts involve differently structured carbonate species. Compared with Fig. 2B, Fig. 3 shows that the thermal treatment had a more pronounced effect on samples 1 and 4. In these solids, two

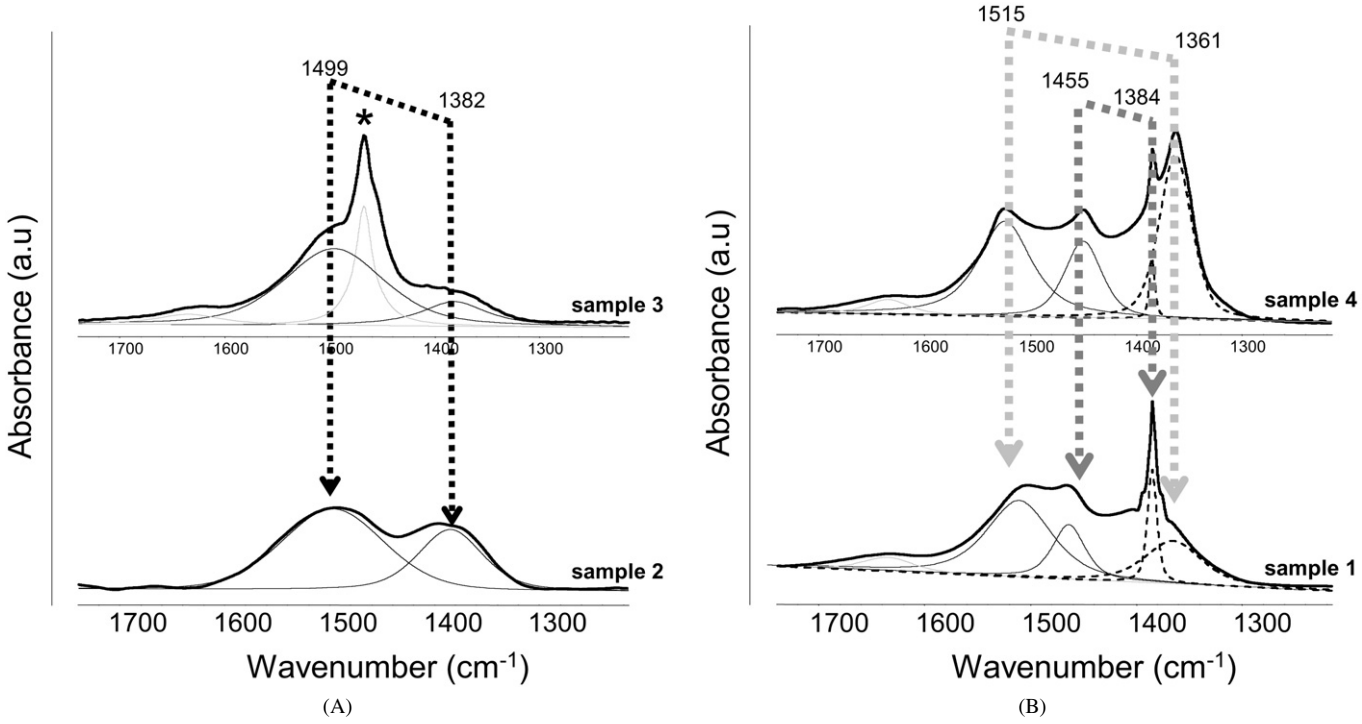

Fig. 3. Main IR decomposition peaks in the ν_3(OCO) range (KBr pellets). (∗) mineral carbonates type II, $La_2O_2CO_3$.

sets of bands, at 1455–1384 and at 1515–1361 cm^{-1}, were resolved. The differences between the band positions in Figs. 2 and 3 are not surprising; the high-temperature treatment in an oxidizing atmosphere carried out before obtaining the spectra certainly strongly modified the carbonates. Hydrogen carbonates, as well as unidentate and bidentate species, were removed, whereas polydentate entities may have changed their coordination and symmetry, as already observed on parent compounds [28]. Moreover, we cannot discard the hypothesis that the spectra observed in Fig. 3 were affected by distortion phenomena due to the sample mixing with KBr [29]. Nevertheless, a tentative interpretation of the observed species can be formulated.

IR spectra of adsorbed carbonates are characterized by the loss of D_{3h} symmetry, which leads to the splitting of the degenerate asymmetric ν_3(OCO) mode. The possibility that the $\Delta\nu_3$ splitting is specific to a given carbonate species structure has been considered; its value was about 100 cm^{-1} for unidentate species, 300 cm^{-1} for bidentate species, and 400 cm^{-1} for bridging species. Unidentate carbonates are currently less stable than bidentates [27]. If a carbonate species shows a strong resistance to thermal treatment and exhibits rather low $\Delta\nu_3$ splitting, it likely corresponds to a polydentate structure [27]. On the basis of such principles and empirical observations, as well as a comparison of the thermal stability of the different species, we assigned the bands at 1455–1384 and 1515–1361 cm^{-1} to polydentate and bidentate carbonates, respectively (Fig. 3 and Table 2). After thermal treatment, the bidentate species were partly removed and transformed into other species detected after high-temperature evacuation (Fig. 2) [27,28], as discussed earlier.

Table 2
Infrared study of basic properties of various lanthanum oxy-carbonate samples

	Propyne adsorption[a] ν(C≡C) (cm^{-1})	CO_3^{2-} assignments (cm^{-1})[b]			
		Minerals[c]	Unidentate carbonates	Bidentate carbonates	Polydentate carbonates
Sample 1	2116			1515 + 1361 (Δ = 154)	1455 + 1384 (Δ = 71)
Sample 2	2117		1499 + 1382 (Δ = 117)		
Sample 3	2118	1465	1499 + 1382 (Δ = 117)		
Sample 4	2115			1515 + 1361 (Δ = 154)	1455 + 1384 (Δ = 71)

[a] Propyne adsorption on La_2O_3 catalysts activated at 373 K.
[b] Carbonate species assignments on samples diluted in KBr powder.
[c] Mineral carbonates type II, $La_2O_2CO_3$ [13].

The aforementioned criteria allowed us to attribute the carbonate bands present in each sample. The results are summarized in Table 2.

After deconvolution of the main peaks occurring in the 1300–1700 cm^{-1} range (KBr spectra, Fig. 3), we can see that the higher the intensity (proportional to the number of sites) of the bands at 1499 and 1382 cm^{-1}, the higher the phytosterol ester yield, independent of the initial rates of the samples. These two bands, probably corresponding to unidentate carbonates, were the most intense in the case of samples 2 and 3, for which the reaction yields were 86 and 89.2%, respectively. In samples 1 and 4, these bands were probably hidden by the bidentate and polydentate bands. This result suggests that unidentate carbonate species were the predominant active species in the selective synthesis of phytosterol esters. Conversely, polydentate

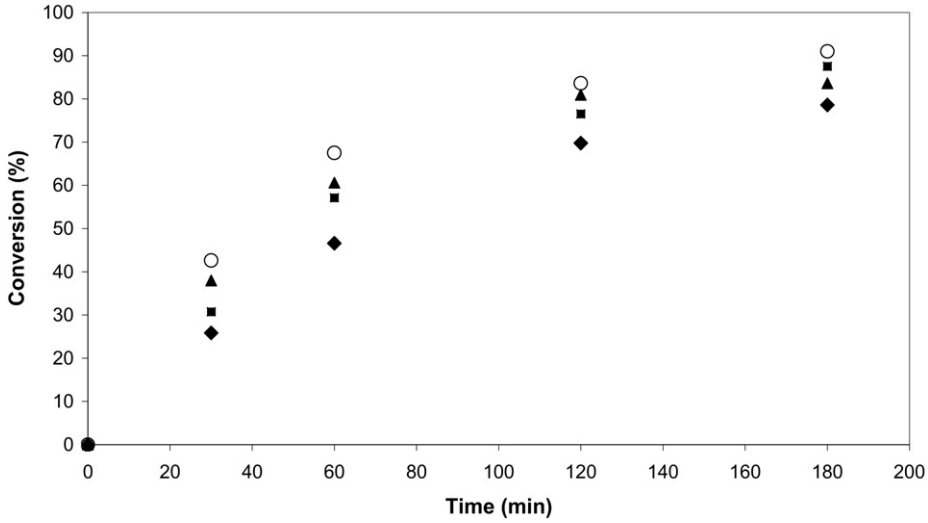

Fig. 4. Sterol conversion as a function of time on stream over various La_2O_3 oxides: (■) sample 1, (◆) sample 2, (▲) sample 3, (○) sample 4.

and bidentate carbonate species, essentially present on the two other samples and characterized by IR bands at 1455–1384 and 1515–1361 cm^{-1}, respectively, were presumably less active for this reaction.

3.3.2. *Catalytic performance of the different La_2O_3 oxides*

Transesterification of the fatty methyl ester with β-sitosterol carried out in the presence of lanthanum oxides led to very high values for the conversion of the ester and sterol and for the selectivity to sterol esters ($\geqslant$90%). Contrary to what was observed for MgO (sterol ester selectivity of 80%) [7], this suggests that the strength of the active basic sites of the various La_2O_3 samples was a determining factor, adapted to the formation of phytosterol ester, the desired product. Indeed, the selectivity to phytosterol ester varied from 89 to 96%, confirming that the side reaction of dehydration of β-sitosterol was substantially limited (formation of side products not exceeding 10%). Thus, the competition between the transesterification reaction and the dehydration of the sterol was highly restricted.

As already mentioned, the most active sample was not the lanthanum oxide with the highest specific surface area (Fig. 4, Table 1), but rather the oxide prepared by the self-combustion method, sample 4 (40 $m^2\,g^{-1}$), and also sample 3 (3 $m^2\,g^{-1}$). This latter sample also was the most selective to phytosterol ester. The high conversion and selectivity values displayed by the various La_2O_3 samples explain an increased yield of phytosterol ester ($\geqslant$83%) compared with other basic oxide catalysts used previously.

Note that for all samples, the selectivity to phytosterol ester was total at zero conversion (at the beginning of the reaction) and decreased slightly continuously as a function of time, down to ~90% (formation of stigmasta-3,5-diene). This means that this side reaction (degradation of reactants) is favored by acid sites that are progressively generated onto the catalyst surface during the reaction. Indeed, the synthesis of phytosterol esters from sterols and fatty methyl esters was accompanied by the formation of methanol. Dehydration of MeOH at 513 K promoted the creation of Brønsted acidity, which was responsible for the formation of dienes by dehydration of β-sitosterol. The absence of Brønsted acid sites on the surface of the various lanthanum oxides was confirmed by adsorption of pyridine and lutidine, which more accurately probes weak Brønsted acid sites.

Pyridine adsorption could be appropriate for checking the coordinative unsaturation of lanthanum at the sample surface. IR spectroscopy of adsorbed pyridine was used to determine the acid type and to probe the acid strength of La_2O_3 samples. Pyridine was adsorbed on lanthanum oxides and further evacuated at room temperature. The adsorption led to the appearance of IR bands at 1618, 1593, 1574, 1486, and 1440 cm^{-1}, all assigned to pyridine coordinated to Lewis acid sites. It is well known that the position and the multiplicity of the ν_{8a} ring vibration of chemisorbed pyridine (1579 cm^{-1} in the liquid phase) is related to the strength and the number of the different types of Lewis acid sites [30]. According to various studies [31–35], the occurrence of the ν_{8a} mode at two different frequency values (1618 and 1593 cm^{-1}) indicates that the Lewis acid sites belong to two different populations with different acidity strengths. As already reported for other oxides [36], the spectra of pyridine chemisorbed on the lanthanum oxide can be interpreted by considering that two types of species are formed, corresponding to La^{3+} in different structural environments (e.g., defects, corners), characterized by the ν_{8a} bands at 1618 and 1593 cm^{-1}.

Whereas the strength of LAS on lanthanum oxide was analyzed from the position of pyridine ν_{8a} absorption bands, their quantification was measured from the area of the ν_{19b} band at about 1440 cm^{-1}, using its molar extinction coefficient (ε = 1.5 μmol^{-1} cm [37]). The total amount of LAS was determined taking into account the area of this band measured after evacuation, so as to eliminate physisorbed and H-bonded pyridine (Table 3). These results show that the lower the specific surface area, the higher the Lewis acid site concentration. Finally, from these results, it appears that the amount of Lewis acid sites present on lanthanum oxides was relatively low, even though pyridine was adsorbed after activating the samples at high temperature. Therefore, under normal reaction conditions, these

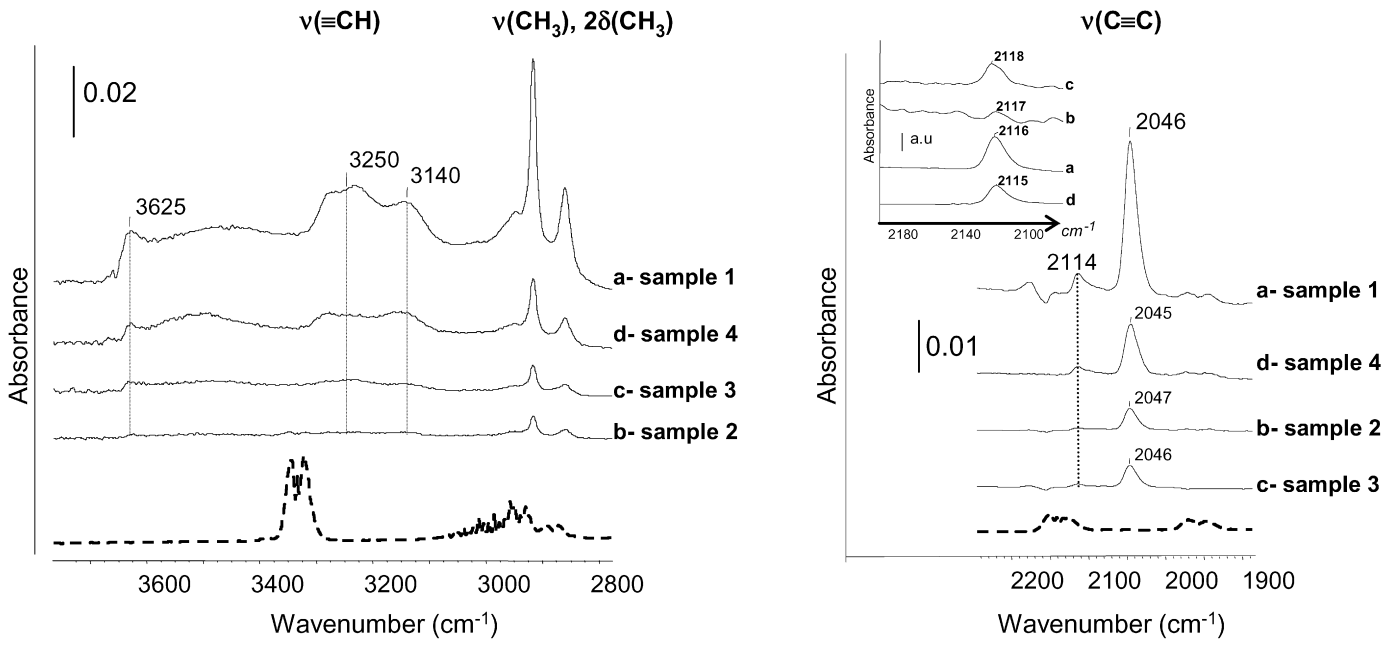

Fig. 5. IR spectra of propyne adsorbed at room temperature (2 Torr at equilibrium) on La_2O_3 samples evacuated at 873 K (dotted line: gas phase). Insert spectra: ν(C≡C) region of propyne adsorbed on La_2O_3 evacuated at 373 K.

Table 3
Lewis acidity of lanthanum oxide catalysts determined from ν_{19b} pyridine adsorption

	Sample 1	Sample 2	Sample 3	La_2O_3 (self combustion)
Area of the band near 1440 cm^{-1}	1.21	0.11	0.14	0.42
n (μmol g^{-1})[a]	40.3	3.7	4.7	14.0
S_{BET} (m^2 g^{-1})	68	1	3	40
C (μmol m^2)	0.6	3.7	1.6	0.4

[a] $A = \varepsilon l(n/Sl) = (\varepsilon n)/S$ with $\varepsilon = 1.5$ μmol^{-1} cm [31], where A, ε, S, n and l denote respectively the absorbance, the integrated molar absorption coefficient, the disc surface, the amount of pyridine adsorbed and the disc thickness.

sites should be occupied by carbonates, and thus they should not have any catalytic efficiency. This explains the high selectivity of lanthanum-based materials and the relative weaker performances of samples 1 and 4, which had the highest concentration of Lewis acid sites and the lowest selectivities.

3.3.3. Correlation between the catalytic performances and the basicity of the La_2O_3 oxides

IR probing of the strength of surface basic sites was carried out by propyne adsorption. As shown by Huber and Knözinger [38] and Mordenti et al. [39], propyne behaves as a C–H acid, which should undergo interaction with basic oxygen centers via H bonding. According to Knözinger and Huber [40] and Michalska et al. [41], C–H acids can be used as probe molecules for basic properties using the H-bonding shift method. The H-bonding stretching frequency can allow ranking of the basic strengths of the La_2O_3 series, because the red shift expected for the C–H stretching mode of adsorbed propyne depends on the basic site strength. Propyne interaction with a surface was studied first by Uvarova et al. [42], who suggested that red shifts indicate the formation of H bonds with framework oxygen atoms. According to Thomasson et al. [43], this σ-complex leads, in the ν(≡CH) stretching vibration range, to the formation of broad bands. Additional bands also could be detected that have been attributed to a π-complex formed between a coordinatively unsaturated cation and the triple bond of propyne. Huber and Knözinger [38] showed that such interaction led to a sharp band on MgO at about 3280 cm^{-1}.

Fig. 5 shows, in the ν(≡CH) and ν(C≡C) range, IR spectra of adsorbed species (difference spectra) formed after adsorption of 2 Torr of propyne on lanthanum-based oxides activated at 873 K under oxygen. As expected, propyne adsorption in the ν(≡CH) range led to the formation of rather broad bands. The $\nu(CH_3)$ and $2\delta(CH_3)$ frequency modes were not shifted relative to gaseous CH_3–C≡CH, indicating that the methyl group of propyne was not perturbed by the adsorption. Adsorption of propyne at room temperature revealed the formation of a new ν(OH) band at 3625 cm^{-1} on the different samples, suggesting partial dissociation of the probe due to the presence of Lewis acid–base pairs [41]. In the ν(≡CH) stretching vibration region, two broad bands at 3250 and 3140 cm^{-1}, red-shifted with respect to the gas-phase frequency (3334 cm^{-1}) by 84 and 194 cm^{-1}, respectively, can be seen in Fig. 5. The occurrence of two different ν(≡CH) frequency values argues for two different molecular adsorption modes. The ν(C≡C) stretching mode corresponding to these (propyne-La_2O_3 surface) complexes were observed at 2114 and 2046 cm^{-1} (sample 1), showing red shifts with respect to the gas-phase frequency of 27 and 98 cm^{-1} (Fig. 5). Evacuation preferentially gave rise to the decrease of the ν(≡CH) broad band at about 3250 cm^{-1}, coupled with the vanishing of the 2115 cm^{-1} ν(C≡C) band.

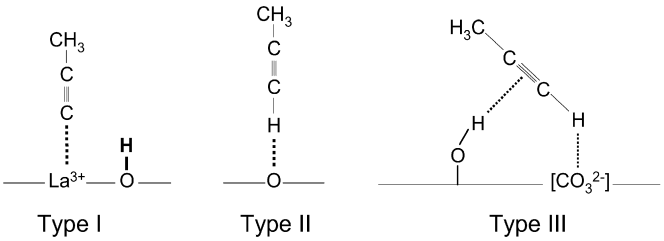

Fig. 6. Possible structures of CH_3–C≡CH adsorbed on lanthanum oxide.

These results clearly demonstrate the presence of two different adsorbed species on lanthanum oxides. Uvarova et al. [42] suggested that a red shift was consistent with the H-bonding interaction and that the decreased ν(CH) values reflected the basic strength of the adsorption sites. In the scheme showing three possible complexes of propyne interacting with the La_2O_3 surface, given in Fig. 6, the strongly held propyne is oriented perpendicularly to the surface (type II), is bonded to basic oxygens, and displays bands at 3140 and 2046 cm^{-1}, whereas the weakly held propyne (type II) is thought to be adsorbed onto carbonate-like surface species (bands at 3250 and 2115 cm^{-1}), likely also in interaction with surface hydroxyls. Finally, a more complete evacuation gave rise to the total elimination of stretching ν(≡CH) vibrations, whereas the ν(C≡C) stretching mode had shifted from 2046 to 2044 cm^{-1} and the band observed at 3625 cm^{-1} was not eliminated. The fact that the ν(C≡C) vibration was observed with no corresponding ν(≡CH) frequency values, coupled with a new ν(OH) band observed at 3625 cm^{-1}, confirms the dissociative adsorption of propyne (type I in Fig. 6). Note that the high-temperature treatment (with partial removal of carbonate species) seemed to favor propyne adsorption on basic oxygens.

To obtain more information on the basic strength of carbonate surface species, propyne also was adsorbed on samples evacuated at 373 K, to avoid an overly extended surface reconstruction, but while reducing the amount of physisorbed water on the sample. The IR spectra are presented in the insert of Fig. 5 and reported in Table 2. Propyne adsorption led to the appearance of ν(C≡C) bands at 2115, 2116, 2117, and 2118 cm^{-1} on samples 4, 1, 2, and 3, respectively. This result demonstrates that all samples involve carbonate species of slightly different strength. The corresponding spectra show that the lower the ν(C≡C) vibration, the higher its carbonate species basicity. The shift expected for the ν(C≡C) propyne stretching mode is depending on the nature of the adsorption sites and its basic strength, indicating that this molecule is a sensitive probe of the basic properties of carbonate species. This difference in basic strength of carbonates species can be directly related to the catalytic efficiency of the lanthanum oxide samples, as shown in Fig. 7. Indeed, the maximum yield obtained for the lanthanum oxide catalysts increased with decreasing carbonate basicity.

As observed in sample 4, overly strong basic sites are not the most active species in the synthesis of phytosterol esters. This means that this reaction requires carbonate species of medium basic strength with a rather ionic character but limited stability (unidentate species), as was observed for sample 3. We can imagine that the catalytic scheme represented in Fig. 1 corresponds to an interaction between the sterol molecule H-bonded to the surface carbonates and the methyl ester via the –COO function. In fact, the unidentate carbonate can be considered merely as a CO_2 molecule chemically bound to a surface, as presented on Scheme 1. Despite the high basicity of the coordination site (an "on top" oxygen over a cation), giving rise to a highly symmetric molecular configuration with a pronounced ionic character, the stability of the complex is very limited due to the lack of coordination [27], therefore favoring catalytic exchange. Conversely, polydentate carbonates have a high intrinsic stability and thus a weak reactivity toward other molecules. Of course, the lability of unidentate species favors the formation of coordinatively unsaturated La^{3+} cations, which act as dehydration sites, thereby justifying the lower selectivity for sample 4 (self-combustion La_2O_3) and sample 1.

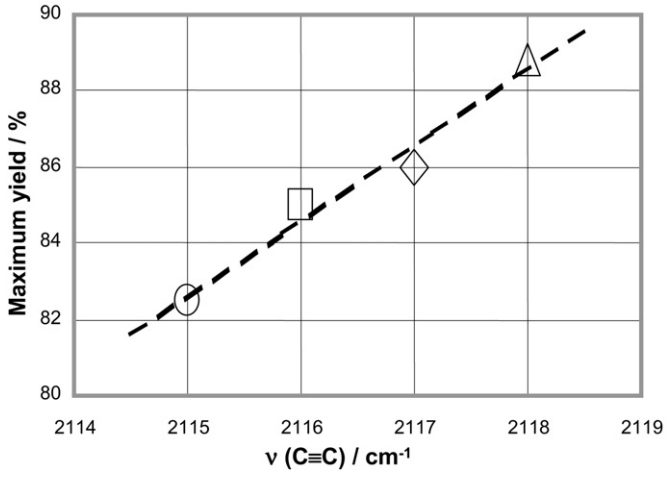

Fig. 7. Correlation between ν(C≡C) and the maximum yield obtained for the lanthanum oxide catalysts: (□) sample 1, (◇) sample 2, (△) sample 3, (○) sample 4.

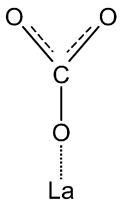

Scheme 1. Schematic representation of a unidentate carbonate on a lanthanum oxide surface.

Finally, the number of basic active sites determined from the total area of the IR propyne bands can be correlated with the activity at zero conversion for all catalysts. Fig. 8 reveals perfect correlation between the initial reaction rate and the total area of the IR bands. The higher the number of carbonate species, the higher the activity determined at zero conversion. On the other hand, because both samples 3 and 4 exhibit the highest (but similar) number of active sites, whereas their corresponding yield of phytosterol ester is different (89.2 and 82.6%, respectively), we can conclude that the strength of the carbonate species is also an important parameter to consider for this catalytic reaction. Consequently, the most competitive catalyst in the transesterification of fatty methyl esters with sterols should

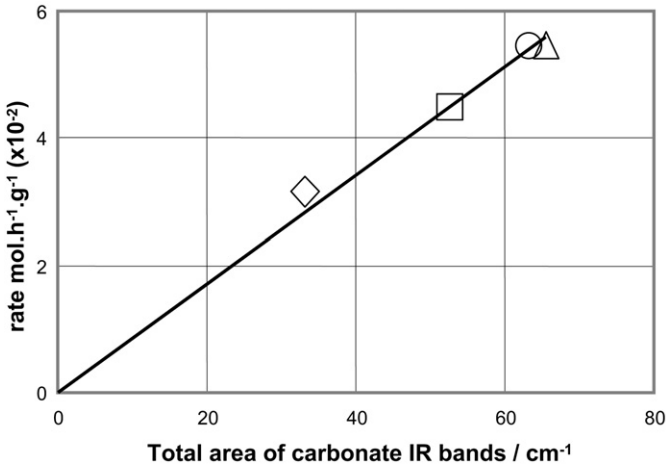

Fig. 8. Correlation between the total area of carbonate IR bands and the activity at zero conversion of lanthanum oxide catalysts: (□) sample 1, (◇) sample 2, (△) sample 3, (○) sample 4.

involve quite ionic carbonate species (e.g., unidentate) with a medium basic strength.

4. Conclusion

The synthesis of phytosterol esters from transesterification of a fatty methyl ester (dodecanoate) with β-sitosterol was carried out in the presence of basic solid catalysts, such as lanthanum oxides, differing in terms of synthesis procedure and specific surface area. These basic oxides proved particularly active and selective to phytosterol esters compared with magnesium oxide or zinc oxide, which were reported previously. The competition between the transesterification reaction and the side reaction of dehydration of sterol was strongly inhibited, resulting in phytosterol ester selectivity of 90–96%. The high conversion and selectivity values displayed by the various La_2O_3 samples led to an increased phytosterol ester yield ($\geqslant$83%) compared with that of other basic oxide catalysts used previously.

The acid–base properties (i.e., nature, number, and strength of active sites) of La_2O_3 were characterized by IR spectroscopy, which revealed the presence of residual carbonate species inside all of the solids. Lanthanum oxide is well known to be very sensitive to CO_2 contained in the ambient atmosphere, leading to partial surface carbonation. After activation of the catalysts at 873 K under O_2, very different surface and structural states of the carbonate-like species were observed by IR spectroscopy, suggesting different basic and catalytic characteristics of the samples. This was substantiated by the fact that no direct relationship between the surface area of the samples and their activity at zero conversion could be derived. Because the catalytic reaction was performed at a relatively low temperature (513 K), all samples were diluted into KBr before the nature of the different carbonate species was characterized. Unidentate, bidentate, polydentate, and mineral carbonates were observed in this La_2O_3 series, and their strengths were determined by propyne adsorption.

Propyne was shown to be a good molecule for probing the basic properties of all of the lanthanum oxycarbonates, because the shift expected for the ν(C≡C) stretching mode depends on the adsorption sites and their basic strength. Propyne adsorption on samples evacuated at 373 K provided more information on the basic strength of the carbonate species. The fact that ν(C≡C) vibrations were observed at different wavenumbers indicated a ranking of the basic strength of the surface carbonates species of the lanthanum oxycarbonate samples. The lower the basicity of carbonates, the higher the phytosterol ester yield. Moreover, a thorough spectral characterization of KBr-diluted samples indicated that the higher the intensity of unidentate carbonate bands (1499 and 1382 cm^{-1}), the higher the sterol ester yield. These results allowed us to propose a tentative mechanistic explanation based on unidentate carbonate species as active sites.

To conclude, the synthesis of phytosterol esters from natural sterols and methyl esters performed in the presence of La_2O_3 catalysts required ionic carbonate species (e.g., unidentate) of medium basic strength.

Acknowledgments

This work was supported by the French Ministry of Economy, Finance and, Industry under the NACACOMO consortium. The authors gratefully acknowledge the Expanscience Laboratory for constructive discussions and their continuous support and Rhodia for supplying lanthanum oxides (samples 1–3).

References

[1] M.P. Van Amerogen, L.C. Lievense, C. Van Hoosten, World patent, WO 98/01126, 15.01.98, Unilever.
[2] I. Wester, J. Ekblom, World patent, WO 99/56558, 11.11.99, Raisio Benecol Oy.
[3] T. Miettinen, H. Vanhanen, I. Wester, US patent, 5 502 045, 26.03.96, Raision Tehtaat Oy.
[4] N. Milstein, M. Biermann, P. Leidl, R. Von Kreis, World patent, WO 99/30569, 24.06.99, Henkel Corp.
[5] O.J. Pollak, Circulation 7 (1953) 702.
[6] D. Burdick, G. Moine, D. Raederstorff, P. Weber, Eur. patent, EP 1004594A1, 31.05.2000, Hoffmann-La Roche AG.
[7] Y. Pouilloux, G. Courtois, M. Boisseau, A. Piccirilli, J. Barrault, Green Chem. 5 (2003) 89.
[8] X. Zhang, A.B. Walters, M.A. Vannice, Appl. Catal. B 4 (1994) 237.
[9] X. Zhang, A.B. Walters, M.A. Vannice, J. Catal. 155 (1995) 290.
[10] S. Lacombe, C. Geantet, C. Mirodatos, J. Catal. 151 (1994) 439.
[11] A. Auroux, A. Gervasini, J. Phys. Chem. 94 (1990) 6371.
[12] B. Veldurthy, J.-M. Clacens, F. Figueras, J. Catal. 229 (2005) 237.
[13] B. Veldurthy, J.-M. Clacens, F. Figueras, Adv. Synth. Catal. 347 (2005) 767.
[14] B. Veldurthy, J.-M. Clacens, F. Figueras, J. Catal. 229 (2005) 237.
[15] R.P. Taylor, G.L. Schrader, Ind. Eng. Chem. Res. 30 (1991) 1016.
[16] B. Klingenberg, M.A. Vannice, Chem. Mater. 8 (1996) 2755.
[17] R.P. Turcotte, J.O. Sawyer, L. Eyring, Inorg. Chem. 8 (1969) 238.
[18] L.R. Pederson, L.A. Chick, G.J. Exarhos, US patent, 5 114 702, 16.10.90, to Battelle Memorial Institute.
[19] G.A.H. Mekhemer, Phys. Chem. Chem. Phys. 4 (2002) 5400.
[20] A. Laachir, V. Perrichon, A. Badri, J. Lamotte, J.C. Lavalley, G.N. Sauvoin, J. Chem. Soc. Faraday Trans. 87 (1991) 1601.
[21] C. Clay, S. Haq, A. Hodgson, Chem. Phys. Lett. 388 (2004) 89.

[22] G. Velazquez, A. Herrera-Gomez, M.O. Martin-Polo, J. Food Eng. 59 (2003) 79.
[23] B. Klingenberg, M.A. Vannice, Appl. Catal. B 21 (1999) 19.
[24] M.P. Rosynek, Catal. Rev. Sci. Eng. 16 (1977) 111.
[25] G. Colon, J.A. Navio, R. Monaci, I. Ferino, Phys. Chem. Chem. Phys. 2 (2000) 4453.
[26] G. Busca, V. Lorenzelli, Mater. Chem. 7 (1982) 89.
[27] E. Payen, J. Grimblot, J.C. Lavalley, M. Daturi, F. Maugé, Application of vibrational spectroscopy in the characterization of oxides and sulfides catalysts, in: J.M. Chalmers, P.R. Griffith (Eds.), Handbook of Vibrational Spectroscopy, vol. 4, Wiley, New York, 2002.
[28] M. Daturi, C. Binet, J.-C. Lavalley, A. Galtayries, R. Sporken, Phys. Chem. Chem. Phys. 1 (1999) 5717.
[29] Z. Gabelica, Bull. Soc. Chim. Belg. 86 (1977) 897.
[30] F. Abbattista, S. Delmastro, G. Gozzelino, D. Mazza, M. Vallino, G. Busca, V. Lorenzelli, G. Ramis, J. Catal. 117 (1989) 42.
[31] G.A.M. Hussein, B.C. Gates, J. Catal. 176 (1998) 395.
[32] G.A.M. Hussein, B.C. Gates, J. Chem. Soc. Faraday Trans. 93 (1996) 2425.
[33] M.I. Zaki, G.A.M. Hussein, S.A. Mansour, H.A. El-Ammay, J. Mol. Catal. 51 (1989) 209.
[34] G. Connel, J.A. Dumesic, J. Catal. 101 (1986) 103.
[35] Y. Nakano, T. Iizuka, H. Hattori, K. Tanabe, J. Catal. 57 (1979) 1.
[36] C. Morterra, S. Coluccia, A. Chiorino, F. Boccuzzi, J. Catal. 54 (1978) 348.
[37] S. Khabtou, T. Chevreau, J.C. Lavalley, Microporous Mater. 3 (1994) 133.
[38] S. Huber, H. Knözinger, J. Mol. Catal. A 141 (1999) 117.
[39] D. Mordenti, P. Grotz, H. Knözinger, Catal. Today 70 (2001) 83.
[40] H. Knözinger, S. Huber, J. Chem. Soc. Faraday Trans. 15 (1998) 2047.
[41] A. Michalska, M. Daturi, J. Saussey, I. Nowak, M. Ziolek, Microporous Mesoporous Mater. 90 (2006) 362.
[42] E.B. Uvarova, L.M. Kustov, V.B. Kazansky, Stud. Surf. Sci. Catal. 94 (1995) 254.
[43] P. Thomasson, O.S. Tyagi, H. Knözinger, Appl. Catal. A 181 (1999) 181.